AGU PUBLICATIONS

Geophysical Research Letters

RESEARCH LETTER
10.1002/2017GL075235

Key Points:
- A new set of nine indicators for the tropical extrema in zonal-mean precipitation is introduced
- Substantial biases in the nine indicators are found in climate simulations
- The ITCZ structure requires at least four indicators for an accurate description

Supporting Information:
- Supporting Information S1

Correspondence to:
M. Popp,
mpopp@princeton.edu

Citation:
Popp, M., & Lutsko, N. J. (2017). Quantifying the zonal-mean structure of tropical precipitation. *Geophysical Research Letters*, *44*, 9470–9478. https://doi.org/10.1002/2017GL075235

Received 8 AUG 2017
Accepted 9 SEP 2017
Accepted article online 15 SEP 2017
Published online 30 SEP 2017

Quantifying the Zonal-Mean Structure of Tropical Precipitation

M. Popp[1] **and N. J. Lutsko**[1]

[1] Program in Atmospheric and Oceanic Sciences, Princeton University, Princeton, NJ, USA; located at NOAA GFDL, Princeton, NJ

Abstract The tropical zonal-mean precipitation in climate models is well known to have substantial biases such as an erroneous double intertropical convergence zone in the Pacific, but a comprehensive quantification of these biases is currently missing. Therefore, we introduce a set of nine indicators that fully characterize the position and magnitude of the tropical extrema in zonal-mean precipitation. An analysis of the Coupled Model Intercomparison Project (CMIP) historical and Atmospheric Model Intercomparison Project (AMIP) simulations reveals large biases in the position and, especially, in the magnitude of the zonal-mean precipitation extrema in both sets of simulations relative to observations. We find some of the nine indicators to be correlated, and that the structure of tropical precipitation can be well represented using four indicators, though these indicators are different in AMIP and CMIP. Previously defined indicators can only partly explain the biases, and so the more comprehensive terminology introduced here is a useful tool for characterizing tropical precipitation.

1. Introduction

The modern climatological mean of Earth's zonal-mean precipitation has a complex structure in the tropics. The most prominent features are a pronounced maximum in the Northern Hemisphere; a secondary, smaller maximum in the Southern Hemisphere; a local minimum close to the equator; and two pronounced subtropical minima (Figure 1). Most climate models capture these features qualitatively but exhibit substantial biases and intermodel spread in the position and, especially, in the magnitude of the extrema in zonal-mean precipitation (Figure 1). However, a consistent and comprehensive terminology for quantifying the biases and the spread in modeled tropical zonal-mean precipitation is still missing, which has made identifying the reasons for these model deficiencies difficult. We address this problem by introducing and analyzing a set of nine indicators that fully characterize the precipitation extrema in the tropics.

Previous studies have characterized aspects of the tropical precipitation in models, observations, or reanalysis using empirical orthogonal functions (Li & Xie, 2014; Lintner et al., 2016), the "tropical precipitation asymmetry index" (Adam, Schneider, et al., 2016; Hwang & Frierson, 2013; Xiang et al., 2017), the "equatorial precipitation index" (Adam et al., 2016), spatial correlations in precipitation between models and observations (Zhang et al., 2015), or simply by determining the position (e.g., Gruber, 1972; Mechoso et al., 1995; Lin, 2007) and the width (Dias & Pauluis, 2011; Byrne & Schneider, 2016b) of the Intertropical Convergence Zone (ITCZ). We define here the ITCZ as the region of the maxima in zonal-mean precipitation. On a regional scale, Stanfield et al. (2016) used several metrics to characterize the North Pacific ITCZ, such as its width, its centerline position, and its magnitude. A number of studies have evaluated the influence of different drivers on the position of the ITCZ (e.g., Adam et al., 2016a, 2016b; Bischoff & Schneider, 2014, 2016; Harrop & Hartmann, 2016; Kang et al., 2008; Möbis & Stevens, 2012; Philander et al., 1996; Popp & Silvers, 2017; Vellinga & Wood, 2002) and the width of the ITCZ (Byrne & Schneider, 2016a); however, the absence of a suitable terminology for describing the tropical zonal-mean precipitation has led to a lack of clarity.

A good example of this problem is the so called "double-ITCZ" bias: The zonal and climatological mean precipitation tends to be too large at the Southern Hemisphere tropical maximum and this maximum tends to lie too far from the equator (Lin, 2007; Li & Xie, 2014; Mechoso et al., 1995). Intuitively, the double-ITCZ bias involves several different (though possibly related) issues, such as the distance between the two peaks, the magnitude of each of the individual peaks, and the differences in precipitation between the two maxima and the equatorial minimum. Previous studies have often not clearly defined what they refer to as double-ITCZ bias and often have been referring to only a single aspect of the problem. The lack of clear definitions

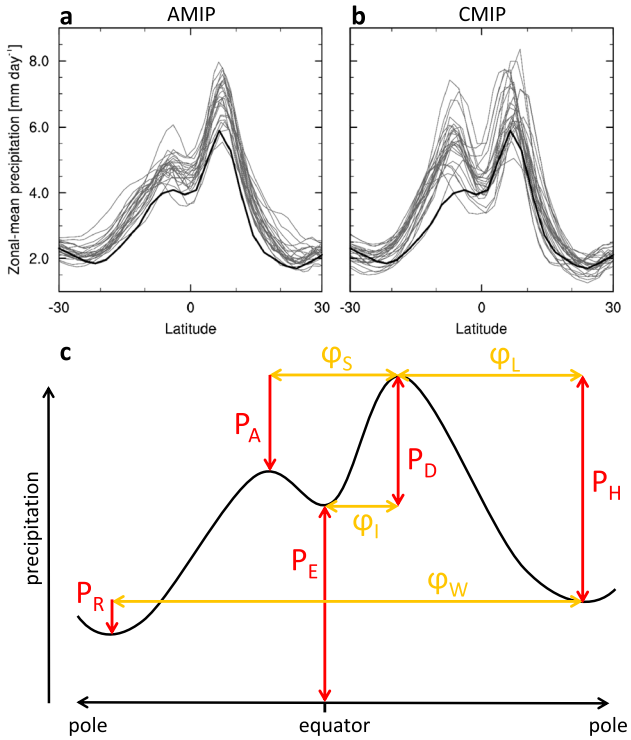

Figure 1. Zonal-mean structure of the climatological mean tropical precipitation. (a) The zonal-mean precipitation in the AMIP simulations with 24 different models (gray lines) over the period from 1979 to 2005. (b) The same but for the historical CMIP simulations with 26 different models (gray lines). The zonal-mean precipitation from the GPCP observations over that same period is shown in black in Figures 1a and 1b. (c) A schematic of the tropical zonal-mean precipitation with the nine indicators defined in section 2.1.

and the use of different indicators in different studies to characterize the double-ITCZ bias has made it difficult to understand what aspects of the problem have been addressed and also to compare studies.

We believe that the nine indicators introduced here will help clarify this discussion and simplify the task of identifying the causes of the biases. The indicators will also be useful for describing the results of less Earth-like simulations, such as idealized aquaplanet configurations or simulations of planetary atmospheres. Below, we define the indicators and then analyze their means, standard deviations, and root-mean-square errors (RMSEs) relative to observations in two multimodel ensembles of simulations (Coupled Model Intercomparison Project (CMIP) historical and Atmospheric Model Intercomparison Project (AMIP)). We also investigate the relationships between the indicators, as well as their ability to reproduce the zonal-mean precipitation. Finally, we compare the nine indicators introduced in this manuscript with previously defined indicators of tropical zonal-mean precipitation.

2. Methods

2.1. Indicators

We choose the nine indicators of the tropical structure of the zonal-mean precipitation shown in Figure 1c. Five of the indicators have units of precipitation. The first of these five indicators is the precipitation amount at the equator. The remaining four are expressed as differences in precipitation amount between two latitudes, with (as ordered here) those latitudes generally moving farther poleward. More specifically, the five indicators are the zonal-mean precipitation at the equator

$$P_E := \bar{P}^{\lambda}(\varphi = 0) \quad , \tag{1}$$

the difference in zonal-mean precipitation between the absolute maximum and the equator

$$P_D := \bar{P}^{\lambda}_{\max} - \bar{P}^{\lambda}(\varphi = 0) \quad , \tag{2}$$

the difference in zonal-mean precipitation between the largest local maxima in each hemisphere,

$$P_A := \bar{P}^{\lambda}_{\mathrm{lmaxNH}} - \bar{P}^{\lambda}_{\mathrm{lmaxSH}} \quad , \tag{3}$$

the difference in zonal-mean precipitation between the absolute maximum and the subtropical minimum in the same hemisphere

$$P_H := \bar{P}^{\lambda}_{\max} - \bar{P}^{\lambda}_{\mathrm{minEHST}} \tag{4}$$

and the difference in zonal-mean precipitation between the subtropical minima in each hemisphere

$$P_R := \bar{P}^{\lambda}_{\mathrm{minNHST}} - \bar{P}^{\lambda}_{\mathrm{minSHST}} \quad , \tag{5}$$

where λ is the longitude and overlines with λ denote zonal means. φ is the latitude, P the precipitation, $P_{\max}$ the maximum in precipitation, and P_{lmaxNH} and P_{lmaxSH} the largest local maximum in precipitation of the Northern and the Southern Hemispheres between the equator and the subtropical minima. P_{minST} denotes the absolute subtropical minimum in precipitation, and P_{minNHST} and P_{minSHST} the minimum in precipitation of the Northern and Southern Hemisphere subtropics, respectively. $P^{\lambda}_{\mathrm{minEHST}}$ denotes the subtropical minimum that is in the same hemisphere as the absolute maximum of precipitation.

The other four indicators have units of latitude. These are the distance in latitude of the absolute maximum zonal-mean precipitation from the equator

$$\varphi_I := \left| \left\{ \varphi \mid \bar{P}^{\lambda}(\varphi) = \bar{P}^{\lambda}_{\max} \right\} \right| \quad , \tag{6}$$

the distance in latitude between the absolute maximum and the largest local maximum in zonal-mean precipitation in the other hemisphere

$$\varphi_S := \left| \left\{ \varphi \mid \bar{P}^{\lambda}(\varphi) = \bar{P}^{\lambda}_{\text{max}} \right\} - \left\{ \varphi \mid \bar{P}^{\lambda}(\varphi) = \bar{P}^{\lambda}_{\text{lmaxOH}} \right\} \right| \quad , \tag{7}$$

the distance in latitude between the maximum and the subtropical minimum in the same hemisphere

$$\varphi_L := \left| \left\{ \varphi \mid \bar{P}^{\lambda}(\varphi) = \bar{P}^{\lambda}_{\text{max}} \right\} - \left\{ \varphi \mid \bar{P}^{\lambda}(\varphi) = \bar{P}^{\lambda}_{\text{minEHST}} \right\} \right| \tag{8}$$

and the distance in latitude between the northern and southern subtropical minima in zonal-mean precipitation

$$\varphi_W := \left| \left\{ \varphi \mid \bar{P}^{\lambda}(\varphi) = \bar{P}^{\lambda}_{\text{minNHST}} \right\} - \left\{ \varphi \mid \bar{P}^{\lambda}(\varphi) = \bar{P}^{\lambda}_{\text{minSHST}} \right\} \right| \quad , \tag{9}$$

where P_{lmaxOH} denotes the largest tropical local maximum in the opposite hemisphere of the absolute maximum in zonal-mean precipitation.

If P_A is positive (negative) the absolute maximum in zonal-mean precipitation is in the Northern (Southern) Hemisphere. If P_R is positive (negative) the absolute subtropical minimum in zonal-mean precipitation is in the Southern (Northern) Hemisphere. If there is no tropical local maximum in the opposite hemisphere, then we define φ_S to be zero, P_A to be equal to P_D if the maximum precipitation is in the Northern Hemisphere, and P_A to be equal to $-P_D$ if the maximum precipitation is in the Southern Hemisphere. If P_A is zero and φ_S is not zero, then φ_I is defined as the distance between the Northern Hemisphere maximum and the equator. If the absolute maximum in precipitation lies exactly at the equator, then P_H is defined as the difference between the absolute maximum and absolute minimum in zonal-mean precipitation and φ_L as the distance between the two extrema. If P_R is zero as well then φ_L is defined as the distance between the absolute maximum and the Northern Hemisphere minimum in zonal-mean precipitation.

Many other indicators could be defined in order to describe the tropical extrema of zonal-mean precipitation. However, we think that it is important for the indicators to smoothly capture both double- and single-ITCZ cases. For instance, if the location and magnitude of the maximum precipitation in each hemisphere were used as indicators, then two of these indicators would not be defined in single-ITCZ cases. Similarly, we choose P_E to be the precipitation at the equator, rather than at the minimum in the deep tropics, because P_E is defined in a single-ITCZ case. It is also useful for certain aspects of the precipitation to be expressed by a single indicator. For example, φ_S is defined so as to directly indicate whether there is one ($\varphi_S = 0$) or two ITCZs ($\varphi_S \neq 0$), while the signs of P_A and P_R indicate the hemispheres in which the maximum and minimum precipitation lie, respectively. By comparing the difference in precipitation between the absolute maximum and the subtropical minimum in the same hemisphere, P_H is related to the strength of the Hadley circulation in that hemisphere. Similarly, φ_L is related to the width of the Hadley cell in that hemisphere, and φ_W to the total width of the Hadley circulation.

The nine indicators are defined such that there is a bijective mapping from the indicators to the magnitude and latitude of the extrema in tropical precipitation (supporting information Text S1).

2.2. Models and Data

We calculate the nine indicators for the CMIP historical simulations (henceforth "CMIP") of 26 models and for the AMIP simulations of 24 models all taking part in the Coupled Model Intercomparison Project phase 5 (CMIP5). We determine the locations of extrema from grid point values without interpolation between grid points. CMIP simulations include dynamical ocean models whereas in AMIP simulations the sea surface temperatures and sea ice are prescribed. We calculate the indicators for the period from 1979 to 2005. The models analyzed in this study are listed in the supporting information Table S1.

For comparison, we also calculate the indicators for the Global Precipitation Climatology Project (GPCP) data for the period from 1979 to 2005 (Adler et al., 2003; Huffman et al., 2009), and for the precipitation obtained from the European Center for Medium-Range Weather Forecasts Interim Reanalysis (ERA-I) for the same time period (Dee et al., 2011).

Table 1
Performance of the Indicators in CMIP and AMIP Simulations, Observations, and Reanalysis

	P_E (mm d^{-1})	P_D (mm d^{-1})	P_A (mm d^{-1})	P_H (mm d^{-1})	P_R (mm d^{-1})	φ_I (deg)	φ_S (deg)	φ_L (deg)	φ_W (deg)
				Observations and Reanalysis					
GPCP	4.02	1.88	1.81	4.20	−0.15	6.25	10.00	17.50	45.00
ERA-I	4.95	2.62	2.26	5.51	0.17	6.75	11.25	18.00	48.75
				AMIP					
Mean	4.53	2.38	2.02	4.95	−0.15	7.03	11.15	17.94	50.14
SD	0.40	0.73	0.66	0.65	0.10	0.54	1.55	2.38	3.45
	9%	30%	33%	13%	63%	8%	13%	13%	7%
				CMIP					
Mean	4.35	2.44	1.02	5.02	−0.28	6.87	13.42	17.32	48.70
SD	0.54	0.87	1.10	0.79	0.23	1.14	2.14	2.12	3.45
	12%	36%	107%	16%	82%	17%	16%	12%	7%
				Bias Relative to GPCP					
RMSE AMIP	0.65	0.87	0.68	0.99	0.09	0.93	2.14	2.37	6.15
	16%	46%	37%	24%	60%	15%	21%	14%	14%
RMSE CMIP	0.62	1.02	1.33	1.13	0.25	1.28	4.01	2.09	5.02
	16%	54%	74%	27%	165%	20%	40%	12%	11%
				Bias Relative to ERA-I					
RMSE AMIP	0.58	0.75	0.69	0.85	0.33	0.60	1.54	2.32	3.65
	12%	29%	30%	16%	200%	9%	14%	13%	8%
RMSE CMIP	0.80	0.87	1.64	0.91	0.50	1.13	3.02	2.19	3.39
	16%	33%	73%	17%	290%	17%	27%	12%	7%

Note. The considered time period is 1979 to 2005. The nine indicators are indicated in the first row. The first column indicates the considered quantity. SD denotes the standard deviation from the multimodel mean. The RMSE is the root-mean-square error of the multimodel ensemble with respect to observations (GPCP) or reanalysis (ERA-I) for the different indicators. The units are indicated in the top row below the variables. We indicate the SD relative to the multimodel mean in percent below the SD values. We indicate the RMSE relative to the observations and reanalysis in percent below the RMSE values.

3. Results

3.1. Magnitude, Variance, and Accuracy of the Indicators in CMIP and AMIP Simulations

The multimodel mean, the standard deviation, and the performance of the models compared to GPCP and ERA-I for the nine indicators are shown in Table 1 for AMIP and CMIP simulations. Overall, the RMSE is smaller for the AMIP simulations than for the CMIP simulations, and in general, the relative RMSE is larger for the indicators related to the magnitude of the precipitation at the extrema (P_E, P_D, P_A, P_H, and P_R) than for the four related to the position of the extrema (φ_I, φ_S, φ_L, and φ_W). That φ_S, P_D, and P_A have large relative RMSEs in both sets of simulations is indicative of the substantial biases in the ITCZ structure present in the models. In general, the RMSEs of the indicators are smaller with respect to ERA-I than for GPCP, with the notable exception of P_R for which the RMSE is much larger for ERA-I. P_R calculated from GPCP has the opposite sign of that calculated from ERA-I, because the absolute subtropical minimum of precipitation lies in the Northern Hemisphere in ERA-I and in the southern in GPCP. Despite the large biases in some of the indicators, only the P_R calculated from ERA-I is outside of the 95% confidence interval (calculated with a *t* test) of both CMIP and AMIP. All other indicators are not significantly different between the models and GPCP and ERA-I, due to the large spread among the models.

The model spread is larger for CMIP than for AMIP for all indicators except φ_L and φ_W. The standard deviation relative to the multimodel mean is especially large for P_A in CMIP, because the standard deviation itself is large and because the multimodel mean strongly underestimates P_A. This, together with φ_S being close to $2\varphi_I$ in CMIP, indicates a more symmetric double ITCZ in CMIP simulations. The subtropical minima, however, appear to be more asymmetric in the CMIP than in the AMIP simulations, because the absolute value of P_R is larger in

Table 2
Squares of the Correlation Coefficients Between the Nine Indicators

	P_E	P_D	P_A	P_H	P_R	φ_I	φ_S	φ_L	φ_W	E_p	A_p	M_p
						AMIP 1979–2005						
P_E	1	**0.23**	0.09	0.02	0.01	0.00	**0.53**	0.03	0.02	**0.61**	0.02	0.08
P_D	**0.23**	1	**0.82**	**0.58**	0.07	0.02	0.10	0.00	0.07	**0.35**	0.01	0.12
P_A	0.09	**0.82**	1	**0.68**	0.13	0.01	0.02	0.03	0.20	0.10	0.04	0.04
P_H	0.02	**0.58**	**0.68**	1	0.20	0.01	0.04	0.09	**0.29**	0.00	0.01	0.13
P_R	0.01	0.07	0.13	0.20	1	0.00	0.01	**0.26**	0.18	0.01	0.08	0.00
φ_I	0.00	0.02	0.01	0.01	0.00	1	0.15	0.15	0.11	0.02	0.01	0.15
φ_S	**0.53**	0.10	0.02	0.04	0.01	0.15	1	0.02	0.05	**0.47**	0.00	0.01
φ_L	0.03	0.00	0.03	0.09	**0.26**	0.15	0.02	1	**0.78**	0.14	0.09	0.15
φ_W	0.02	0.07	0.20	**0.29**	0.18	0.11	0.05	**0.78**	1	0.10	0.01	0.08
						CMIP 1979–2005						
P_E	1	**0.25**	0.05	0.02	0.00	**0.27**	**0.54**	0.07	**0.33**	**0.76**	0.04	0.10
P_D	**0.25**	1	**0.59**	**0.56**	0.08	0.07	0.17	0.01	0.01	**0.29**	0.16	0.05
P_A	0.05	**0.59**	1	**0.51**	0.01	0.03	0.07	0.10	0.02	0.01	**0.36**	0.01
P_H	0.02	**0.56**	**0.51**	1	0.07	0.00	0.00	0.16	0.10	0.00	0.14	0.14
P_R	0.00	0.08	0.01	0.07	1	0.00	0.01	0.05	0.01	0.03	0.04	0.10
φ_I	**0.27**	0.07	0.03	0.00	0.00	1	**0.73**	0.00	**0.27**	**0.29**	0.05	0.00
φ_S	**0.54**	0.17	0.07	0.00	0.01	**0.73**	1	0.00	**0.29**	**0.51**	0.08	0.01
φ_L	0.07	0.01	0.10	0.16	0.05	0.00	0.00	1	**0.56**	0.05	0.00	0.01
φ_W	**0.33**	0.01	0.02	0.10	0.01	**0.27**	**0.29**	**0.56**	1	**0.31**	0.05	0.03

Note. The squares of the correlation coefficients between the nine indicators and the equatorial precipitation index (E_p), the tropical precipitation asymmetry (A_p), and the tropical-mean precipitation (M_p) from 20S to 20N are also shown. The square of the correlation coefficients corresponds to the coefficient of determination (also "R^2") and indicates how much of the variance between the variables is explained. The top 10 rows refer to the AMIP simulations and the bottom 10 rows to the CMIP simulations. Correlations that have a two-sided p value of less than 0.025 are in bold print and are defined to be statistically significant. Note that the indicators are perfectly autocorrelated and that the correlation is symmetric.

the CMIP simulations. There are no substantial differences in the multimodel means of P_E, P_D, P_H, φ_I, φ_L, and φ_W between AMIP and CMIP simulations. The multimodel means in AMIP and CMIP overestimate P_E, P_D, and P_H relative to GPCP but underestimate these indicators relative to ERA-I.

Outliers, defined as indicator values that lie more than two standard deviations from the mean, were found for φ_S and P_D with one model (CSIRO-Mk3-6-0) and for φ_L in another model (ACCESS1-3) in the CMIP simulations. Two models (FGOALS-s2 and IPSL-CM5A-LR) had anomalously large φ_S in the AMIP simulations. The spread in indicator values across models is not dominated by outliers.

3.2. Relation Between the Indicators

We expect a few indicators, such as P_E and P_D, P_D and P_H, P_D and P_A, and φ_I and φ_S to be somewhat correlated, due to the definition of these quantities as differences in latitude or in precipitation. Indeed, P_D and P_H and P_D and P_A are strongly correlated in both AMIP and CMIP simulations, because the variances of P_H and P_A are dominated by the variance in P_D (Table 2). P_A and P_H are even more strongly correlated in AMIP simulations with almost 80 % of the variance explained. However, the correlation between P_E and P_D is considerably lower, with only about a quarter of the variance of P_D explained by the variance of P_E in both CMIP and AMIP. Surprisingly, φ_S is highly correlated with P_E with about half the variance explained in both CMIP and AMIP. That is, the distance between the two tropical precipitation maxima is well correlated across models with the precipitation at the equator.

In general, more indicators are correlated in CMIP, with 11 out of the 36 possible correlations between the indicators (not accounting for autocorrelations) being statistically significant, compared to only 8 out of the 36 in AMIP. The largest single difference between CMIP and AMIP simulations is that φ_I (the distance between the latitude of maximum precipitation and the equator) and φ_S are very highly correlated in CMIP but not in

AMIP. The CMIP models also have notably stronger correlations than the AMIP models between P_E and φ_I, P_E and φ_W, and φ_S and φ_W.

3.3. Predictive Skill

To further demonstrate the relevance of the indicators, as well as to determine which indicators are the most relevant for capturing the intermodel spread in tropical precipitation, we have used the indicators to predict the zonal-mean tropical precipitation in the models. To do this, nine basis functions were obtained by linear regression of the indicators to the climatological zonal-mean precipitation at each latitude. That is, we calculated the nine functions that minimize the quantity

$$\epsilon(\varphi) := \sqrt{\frac{1}{N}\sum_{m=1}^{N}\left(\bar{P}^{\lambda}(\varphi,m) - \sum_{J\in\{P_E,P_D,P_A,P_H,P_R,\varphi_I,\varphi_S,\varphi_W,\varphi_L\}} f_J(\varphi)J(m)\right)^2}\quad , \tag{10}$$

where m denotes the model, N the number of models in the ensemble, $J(m)$ denotes the value of the indicator J of the model m, and f_J denotes the basis function of the indicator J. The tropical precipitation can then be approximated by multiplying the functions by their corresponding indicator and summing

$$\bar{P}^{\lambda}(\varphi,m) \approx \sum_{J\in\{P_E,P_D,P_A,P_H,P_R,\varphi_I,\varphi_S,\varphi_W,\varphi_L\}} f_J(\varphi)J(m)\quad . \tag{11}$$

Comparing the RMSE between the models' tropical precipitation and the predicted tropical precipitation, the small values across the tropics suggest a good prediction for AMIP (supporting information Figure S1, left column). Almost the same quality of prediction is obtained using only the six indicators P_E, P_D, P_A, P_H, φ_L, and φ_W, and even with only the four indicators P_E, P_D, P_H, and φ_W the prediction is still good. Note that the sets of indicators P_E, P_D, P_A, and φ_W as well as P_E, P_D, P_H, and φ_L give almost an identical quality of prediction. We have found that a reasonable prediction can still be obtained with a linear regression of the three indicators P_E, P_D, and φ_W. The standard deviation of the predicted precipitation is, however, considerably smaller poleward of the ITCZs than that of the multimodel ensemble in this case. This suggests that in AMIP simulations, the spread across models in the zonal-mean precipitation can be represented in the deep tropics with the indicators P_E, P_D, and φ_W, and in the entire tropics with the indicators P_E, P_D, P_H, and φ_W (or P_E, P_D, P_A, and φ_W, or P_E, P_D, P_H, and φ_L).

The RMSE is generally larger for the prediction of the CMIP precipitation (supporting information Figure S1, right column) than for the prediction of the AMIP precipitation (supporting information Figure S1, left column), but overall, the prediction with nine indicators is still reasonably good. The prediction underestimates the model spread on the poleward flank of the Northern Hemisphere ITCZ, and accordingly, the RMSE is also large in that region. Using only the six indicators P_E, P_D, P_A, P_H, φ_S, and φ_W deteriorates the quality of prediction in the Southern Hemisphere subsidence region and on the poleward flank of the Northern Hemisphere ITCZ. Replacing φ_S by P_R improves the prediction in the Southern Hemisphere subsidence region but deteriorates the prediction at lower latitudes. A reasonable prediction of the multimodel ensemble can be obtained in the deep tropics with the four indicators P_E, P_D, P_A, and φ_S. Unlike for AMIP, it is not possible to obtain a decent prediction of the Southern Hemisphere precipitation in the CMIP models with only three indicators. Since these four indicators (P_E, P_D, P_A, and φ_S) quantify the magnitudes and relative positions of the maxima in precipitation, it is doubtful that an accurate description of the ITCZ structure in CMIP simulations can be attained by any further simplification.

Comparing with the AMIP results, the greater spread in the positions and magnitudes of the tropical precipitation maxima in the CMIP simulations means that P_A, P_D, and φ_S are more relevant for capturing the model spread in tropical precipitation in coupled simulations. In AMIP simulations there is less spread in the precipitation maxima and so different indicators can be used to reproduce the profile of tropical precipitation. This picture is consistent with the results obtained by Li and Xie (2014) and Lintner et al. (2016) who find that in the tropical Pacific there is larger spread in the position and width of the ITCZ in CMIP than in AMIP simulations, but that substantial biases in the amount of precipitation remain in AMIP. In particular, Li and Xie (2014) also find that more than half the variance between models in precipitation in the tropical Pacific is associated with the double-ITCZ bias in the CMIP simulations.

4. Discussion and Conclusions

4.1. Comparison With Other Indicators

Several previous studies have linked the zonal-mean double-ITCZ structure of precipitation in CMIP and observations to the tropical hemispherical asymmetry in precipitation (e.g., Hwang & Frierson, 2013; Xiang et al., 2017) using the "tropical precipitation asymmetry index":

$$A_p = \frac{\bar{P}^{\,0S-20N} - \bar{P}^{\,20S-0S}}{\bar{P}^{\,20S-20N}} \quad , \tag{12}$$

where overlines denoted with latitudes are area means over the region between the two indicated latitudes. There is no clear link between the tropical precipitation asymmetry index and any of the nine indicators (Table 2), however. This suggests that the precipitation extrema, and thus, the ITCZ structure, cannot accurately be described by the hemispherical asymmetry in precipitation alone. But this also means that none of the nine indicators on their own can describe the hemispheric asymmetry in precipitation, which is a useful quantity. A multiple linear regression with all nine indicators explains around 66% of the variance of the tropical precipitation asymmetry index across models in CMIP and 53% in AMIP simulations. P_A, φ_I, and φ_L suffice to explain around half the variance of A_p across models in CMIP simulations, whereas in AMIP P_E, P_D, P_A, P_H P_R, and φ_L are necessary to explain around half the variance of A_p. Estimating the tropical precipitation asymmetry with the nine indicators using the trapezoid rule of integration between the extrema to approximate the hemispheric mean of tropical precipitation does not yield high correlations with the actual asymmetry index either (supporting information Text S2 and Table S2).

Adam, Schneider, et al. (2016) suggest that the ITCZ structure may be linked to the "equatorial precipitation index" that relates the equatorial precipitation to the tropical-mean precipitation:

$$E_P = \frac{\bar{P}^{\,2S-2N}}{\bar{P}^{\,20S-20N}} - 1 \quad . \tag{13}$$

The idea is that if the ITCZs are close to the equator, the equatorial precipitation should be large compared to the tropical-mean precipitation and it should be small if the ITCZs are farther away. Our results suggest indeed that the equatorial precipitation index explains about half the variance of φ_S. However, the variance of φ_S is even better explained by the equatorial precipitation alone (P_E). The equatorial precipitation index does a better job at predicting the variance in P_D than does P_E. So overall the equatorial prediction index can explain some but not all of the structure of the ITCZ.

Note that variations in tropical-mean precipitation (M_p) are not strongly linked to any of the indicators. A simplified calculation of the tropical-mean precipitation using the nine indicators is well correlated with M_p (supporting information Text S2 and Table S2).

4.2. Comparison of Indicators Between AMIP and CMIP

How well do the different indicators correlate between AMIP and CMIP simulations? To investigate this, we analyze the twenty models for which both AMIP and CMIP simulations were performed (supporting information Table S1). In general, the indicators describing the subtropical minima are better correlated than the ones describing the ITCZs, but the spread among AMIP simulations cannot explain more than 34 % of the variance of any indicator in the CMIP simulations (and vice versa) (supporting information Table S3). This is in agreement with Li and Xie (2014) who find that the equatorial precipitation in the tropical Pacific does not correlate well between CMIP and AMIP, and that the biases in CMIP are, in general, better correlated with biases in sea surface temperatures than with biases in AMIP simulations. However, the tropical-mean precipitation from 20S to 20N is strongly correlated between AMIP and CMIP models. This raises the question whether some of the correlations between the indicators P_E, P_D, P_A, P_H, and P_R (that indicate magnitudes of precipitation) are caused by the high correlation in tropical-mean precipitation. Therefore, we normalized these five indicators, by dividing them by the tropical-mean precipitation and performed a correlation analysis with the thus normalized indicators. Overall, the normalization does not substantially change the correlation between the indicators, except that the normalized P_H is strongly correlated with φ_W (supporting information Tables S4 and S5). This suggests that there is a relationship between the strength and width of the Hadley circulation in climate models.

4.3. Caveats

The correlations between the indicators were calculated for the period of 1979 to 2005. To test the robustness of the results, we also calculated the correlations for the period 1979 to 2008 in AMIP (supporting information

Table S6) and for the period 1861 to 2005 in CMIP (supporting information Table S7). The correlations differ slightly for CMIP when using the period 1861 to 2005, but the results are qualitatively similar. However, when the AMIP calculations are repeated for the period 1979 to 2008, φ_S and P_E are not strongly correlated anymore. This is because two models (BCC-CSM1-1 and CanAM4) do not exhibit a double ITCZ, and so φ_S is zero for these models. These two models have a very marginal ITCZ in the Southern Hemisphere in the period 1979 to 2005 that vanishes with the three additional years. Note that in observations, there is a clear double ITCZ throughout the period 1979 to 2008. A feature of indicators that describe the existence of ITCZ (such as φ_S) is that if small changes in precipitation make a second ITCZ appear or disappear, large changes in the value of the indicators occur. This suggests that the correlation between φ_S and P_E may be small if both single- and double-ITCZ cases are present in multimodel ensembles. In eight aquaplanet simulations, in which simulations with both and single and double ITCZs exist, φ_S and P_E are, however, correlated and thus suggest that this is not necessarily the case in other setups (supporting information Table S8).

4.4. Conclusions and Summary

We have introduced nine indicators for the tropical zonal-mean precipitation with the aim of creating a unified, comprehensive terminology for describing tropical precipitation. This terminology will allow future studies to refer to the specific aspects of the tropical precipitation that they are addressing and will also allow the results of different studies to be compared more easily. This will allow a more detailed attribution of precipitation biases to model deficiencies or to biases of other quantities in future studies. Our analysis of the indicators in AMIP and CMIP simulations has highlighted a number of deficiencies in the models. For instance, the models tend to do worse at capturing the magnitude of the tropical precipitation than at capturing the position of the extrema. By specifying the SSTs, the AMIP simulations tend to have lower errors relative to observations, but even these simulations have relatively large errors related to the structure of the double ITCZ. We have also uncovered some unexpected relationships between the indicators. Perhaps most notably, the distance between the two ITCZs is strongly correlated with the equatorial precipitation. This correlation holds in both the CMIP and the AMIP data.

A comparison with previously used indicators of precipitation suggests that the hemispheric asymmetry index does not correlate well with the indicators describing aspects of the double-ITCZ structure, whereas the equatorial precipitation index explains about half the variance in the distance between the two ITCZs and about a third of the variance in the difference between the precipitation at the larger ITCZ and the equatorial precipitation. However, a linear regression of the nine indicators to the multimodel ensemble suggests that the full ITCZ structure cannot be accurately captured with less than three indicators in AMIP and four in CMIP. This supports our notion that it is important to consider multiple indicators when discussing the structure of the ITCZ.

Possible future applications of the nine indicators we have defined here include the characterization of the zonal-mean tropical precipitation in specific regions of interest, in different seasons, in simulations of future climate change, in paleoclimate scenarios, and in simulations of less Earth-like climates.

Acknowledgments

We thank Isaac Held and Levi Silvers for thorough internal reviews and many constructive comments and two anonymous reviewers for their constructive and helpful reviews. This report was prepared by Max Popp under award NA14OAR4320106 from the National Oceanic and Atmospheric Administration and U.S. Department of Commerce. The statements, findings, conclusions, and recommendations are those of the authors and do not necessarily reflect the views of the National Oceanic and Atmospheric Administration, or the U.S. Department of Commerce. Nicholas Lutsko was supported by NSF grant DGE 1148900. The data can be downloaded from the CMIP archive. The scripts used to perform the analysis are available at https://github.com/nicklutsko/tropical_precip_indicators.

References

Adam, O., Schneider, T., Brient, F., & Bischoff, T. (2016). Relation of the double-ITCZ bias to the atmospheric energy budget in climate models. *Geophysical Research Letters*, *43*, 7670–7677. https://doi.org/10.1002/2016GL069465

Adam, O., Bischoff, T., & Schneider, T. (2016a). Seasonal and interannual variations of the energy flux equator and ITCZ. Part I: Zonally averaged ITCZ position. *Journal of Climate*, *29*(9), 3219–3230.

Adam, O., Bischoff, T., & Schneider, T. (2016b). Seasonal and interannual variations of the energy flux equator and ITCZ. Part II: Zonally varying shifts of the ITCZ,. *Journal of Climate*, *29*(20), 7281–7293.

Adler, R. F., Huffman, G. J., Chang, A., Ferraro, R., Xie, P.-P., Janowiak, J., … Nelkin, E. (2003). The version-2 global precipitation climatology project (GPCP) monthly precipitation analysis (1979–present). *Journal of Hydrometeorology*, *4*(6), 1147–1167.

Bischoff, T., & Schneider, T. (2014). Energetic constraints on the position of the intertropical convergence zone. *Journal of Climate*, *27*(13), 4937–4951.

Bischoff, T., & Schneider, T. (2016). The equatorial energy balance, ITCZ position, and double-ITCZ bifurcations. *Journal of Climate*, *29*(8), 2997–3013.

Byrne, M. P., & Schneider, T. (2016a). Energetic constraints on the width of the intertropical convergence zone. *Journal of Climate*, *29*(13), 4709–4721.

Byrne, M. P., & Schneider, T. (2016b). Narrowing of the ITCZ in a warming climate: Physical mechanisms. *Geophysical Research Letters*, *43*, 11350–11357. https://doi.org/10.1002/2016GL070396

Dee, D. P., Uppala, S. M., Simmons, A. J., Berrisford, P., Poli, P., Kobayashi, S., … Vitart, F. (2011). The ERA-Interim reanalysis: Configuration and performance of the data assimilation system. *Quarterly Journal of the Royal Meteorological Society*, *137*, 553–597.

Dias, J., & Pauluis, O. (2011). Modulations of the phase speed of convectively coupled Kelvin waves by the ITCZ. *Journal of the Atmospheric Sciences*, *68*(7), 1446–1459.

Gruber, A. (1972). Fluctuations in the position of the ITCZ in the Atlantic and Pacific Oceans. *Journal of the Atmospheric Sciences*, *29*, 193–196.

Harrop, B. E., & Hartmann, D. L. (2016). The role of cloud radiative heating in determining the location of the ITCZ in aquaplanet simulations. *Journal of Climate*, *29*(8), 2741–2763.

Huffman, G. J., Adler, R. F., Bolvin, D. T., & Gu, G. (2009). Improving the global precipitation record: GPCP version 2.1. *Geophysical Research Letters*, *36*, L17808. https://doi.org/10.1029/2009GL040000

Hwang, Y.-T., & Frierson, D. M. W. (2013). Link between the double-Intertropical Convergence Zone problem and cloud biases over the Southern Ocean. *Proceedings of the National Academy of Sciences*, *110*(13), 4935–4940.

Kang, S. M., Held, I. M., Frierson, D. M. W., & Zhao, M. (2008). The response of the ITCZ to extratropical thermal forcing: Idealized slab-ocean experiments with a GCM. *Journal of Climate*, *21*(14), 3521–3532.

Li, G., & Xie, S.-P. (2014). Tropical biases in CMIP5 multimodel ensemble: The excessive equatorial pacific cold tongue and double ITCZ problems. *Journal of Climate*,*27*(4), 1765–1780.

Lin, J.-L. (2007). The double-ITCZ Problem in IPCC AR4 Coupled GCMs: Ocean-atmosphere feedback analysis. *Journal of Climate*, *20*(18), 4497–4525.

Lintner, B. R., Langenbrunner, B., Neelin, J. D., Anderson, B. T., Niznik, M. J., Li, G., & Xie, S.-P. (2016). Characterizing CMIP5 model spread in simulated rainfall in the Pacific Intertropical Convergence and South Pacific Convergence Zones. *Journal of Geophysical Research: Atmospheres*, *121*, 11,590–11,607. https://doi.org/10.1002/2016JD025284

Mechoso, C. R., Robertson, A. W., Barth, N., Davey, M. K., Delecluse, P., Gent, P. R., … Tribbia, J. J. (1995). The seasonal cycle over the tropical Pacific in coupled ocean-atmosphere general circulation models. *Monthly Weather Review*, *123*(9), 2825–2838.

Möbis, B., & Stevens, B. (2012). Factors controlling the position of the intertropical convergence zone on an aquaplanet. *Journal of Advances in Modeling Earth Systems*, *4*(4), M00A04.

Philander, S. G. H., Gu, D., Lambert, G., Li, T., Halpern, D., Lau, N.-C., & Pacanowski, R. C. (1996). Why the ITCZ is mostly north of the equator. *Journal of Climate*, *9*(12), 2958–2972.

Popp, M., & Silvers, L. G. (2017). Single and double ITCZs with and without clouds. *Journal of Climate*, https://doi.org/10.1175/JCLI-D-17-0062.1

Stanfield, R. E., Jiang, J. H., Dong, X., Xi, B., Su, H., Donner, L., … Shindo, E. (2016). A quantitative assessment of precipitation associated with the ITCZ in the CMIP5 GCM simulations. *Climate Dynamics*, *47*(5–6), 1863–1880.

Vellinga, M., & Wood, R. A. (2002). Global climatic impacts of a collapse of the Atlantic thermohaline circulation. *Climatic Change*, *54*(3), 251–267.

Xiang, B., Zhao, M., Held, I. I. M., & Golaz, J.-C. (2017). Predicting the severity of spurious "double ITCZ" problem in CMIP5 coupled models from AMIP simulations. *Geophysical Research Letters*, *44*, 1520–1527. https://doi.org/10.1002/2016GL071992

Zhang, X., Liu, H., & Zhang, M. (2015). Double ITCZ in coupled ocean-atmosphere models: From CMIP3 to CMIP5. *Geophysical Research Letters*, *42*, 8651–8659. https://doi.org/10.1002/2015GL065973